Fluctuation effects of meson fields on quantum hadrodynamics at finite temperature

Ru-Keng Su
China Center of Advanced Science and Technology (World Laboratory), P. O. Box 8730, Beijing, People's Republic of China and Department of Physics, Fudan University, Shanghai, 200433, People's Republic of China

Zhi-Xin Qian
Department of Physics, Fudan University, Shanghai, 200433, People's Republic of China
(Received 22 November 1991)

By means of the real-time Green's functions method with a pair cutoff approximation up to the second order, the thermal fluctuation effects of meson fields on quantum hadrodynamics are investigated. We find that the fluctuation effects of saturation energy, effective mass of nucleon, and the pressure are considerable in low baryon density regions and/or high temperature regions. The results given by pair cutoff theory and by mean field theory are compared.

PACS number(s): 21.60.−n, 21.65.+f

I. INTRODUCTION

A great deal of progress has been made in nuclear theory by carrying out relativistic many-body calculations of the binding energy, equation of state, and other thermodynamical quantities for nuclear matter [1–7]. They include the Dirac phenomenology [1], relativistic nuclear mean field theory (MFT) [2–5], especially, the quantum hadrodynamics (QHD) [3]. QHD can give a good description of many of bulk features of nuclear matter. In high baryon density regions, the results given by MFT of QHD are in good agreement with part of experiments.

There are two models, namely, QHD-I and QHD-II in QHD [3]. The degrees of freedom in QHD-I are baryons and mesons. In this model, the vector mesons (ω mesons) are coupled minimally to the conserved baryon current, and the scalar mesons (σ mesons) are coupled to baryons with Yukawa coupling. Since there is repulsion between two baryons at short distances by ω-meson exchange and attraction at large distances by σ-meson exchange, the dominant features of nuclear force can be simulated by this model. By means of these interactions and MFT, one can find the correct nuclear matter equation of state in high baryon density regions, because the scalar and vector field operators can be replaced by their expectation values in this case and we can solve the equations of motion of baryon fields and meson fields simultaneously. In this paper, we employ the QHD-I model as our starting Lagrangian.

As was pointed out by many references of statistical physics [6], for four-dimensional space-time, MFT is not a good theory for describing the behavior near the critical point. The critical point is the point at which the order parameter of a new phase begins to grow continuously from zero. In the liquid-gas transition, the critical point terminated the liquid-gas coexistence curve. At critical point, the two-body correlations become very strong and the fluctuations become very large. The MFT do not properly take the effects of short-ranged correlations into account at the critical point and then do not give the correct results for critical behavior. It is of interest to study the relativistic fluctuation effects of meson fields, namely, $\langle(\Delta\phi)^2\rangle=\langle\phi^2\rangle-\langle\phi\rangle^2$, $\langle(\Delta V_\mu)^2\rangle=\langle V_\mu^2\rangle-\langle V_\mu\rangle^2$, on the equation of state, the thermodynamical quantities, and the critical phenomena of nuclear matter in QHD. This is the first motivation of our study.

The second motivation of our study is to extend our real-time finite-temperature Green's function method with pair cutoff approximation from nonrelativity to relativity. In a series of previous papers [9–15], we developed a real-time finite-temperature Green's function method to investigate the liquid-gas phase transition of symmetric or asymmetric nonrelativistic nuclear matter with Skyrme interactions as well as Gogny interactions. We focused our attention mainly on discussing the equations of motion of nucleon Green's functions. In order to make the set of hierarchy of Green's functions equations closed, we introduced a normal pair cutoff (PC) approximation and proved that the first-order PC approximation is just the finite temperature Hartree-Fock theory. To investigate the fluctuation effects of mesons on QHD at finite temperature, we first extend our real-time finite-temperature Green's function method to a relativistic case. Furthermore, we introduce the PC approximation up to second order for studying the fluctuations of meson fields $\langle(\Delta\phi)^2\rangle$, $\langle(\Delta V_\mu)^2\rangle$. Using this approach, we can investigate the thermal correlation function of $\langle\phi^2\rangle$ and $\langle V_\mu^2\rangle$, where $\langle\cdots\rangle$ denotes the grand canonical ensemble expectation value and is defined as $\mathrm{Tr}[\cdots\exp(\Omega-\beta\tilde{H})]$, where $\tilde{H}=H-\mu N$, μ and N being, respectively, the chemical potential and the number operator, and Ω is the thermodynamic potential. We will prove that the effective mass of nucleon M^*, the saturation energy, the equation of state of liquid-gas phase transition will have a considerable change in low-density regions and/or in high-temperature regions when the thermal correlation function is taken into account.

The rest of this paper is organized as follows. In Sec.

II we will describe our approach briefly, especially, we will show how to extend our method to relativistic quantum hadrodynamical model QHD-I. In this section, we will use the second-order PC approximation to find the correlation functions $\langle \phi^2 \rangle$, $\langle V_\mu^2 \rangle$ of meson fields. The main formulas for thermodynamical quantities are presented in Sec. III. In Sec. IV we will give our numerical results for effective mass, saturation energy, and equation of state and some discussions.

II. REAL-TIME GREEN'S FUNCTION

Our calculations are based on the framework of the real-time finite-temperature Green's function method. The details of this method can be found in Refs. [9] and [11]. Here we write down some essential steps of this method which are necessary for the present calculations.

Starting from the Lagrangian density of QHD-I [3]:

$$L=\bar{\psi}[\gamma_\mu(i\partial^\mu-g_v V^\mu)-(M-g_s\phi)]\psi+\tfrac{1}{2}(\partial_\mu\phi\partial^\mu\phi-m_s^2\phi^2) -\tfrac{1}{4}F_{\mu\nu}F^{\mu\nu}+\tfrac{1}{2}m_v^2V_\mu V^\mu , \quad (1)$$

where ϕ, V_μ are, respectively, neutral scalar meson field and neutral vector meson field. We get the Hamiltonian density corresponding to the grand canonical ensemble to be

$$\tilde{H}=H-\mu N=\bar{\psi}[i\gamma\cdot\nabla+M-g_s\phi+g_v\gamma_\alpha V^\alpha-\mu\gamma^0]\psi -\partial_0\phi\partial^0\phi-\tfrac{1}{2}\partial_\alpha\phi\partial^\alpha\phi+\tfrac{1}{2}m_s^2\phi^2 +F_{\lambda 0}\partial^0 V^\lambda+\tfrac{1}{4}F_{\alpha\beta}F^{\alpha\beta}-\tfrac{1}{2}m_v^2 V_\alpha V^\alpha , \quad (2)$$

where μ is the chemical potential. The real-time baryon Green's function is defined as

$$G_{\alpha\beta}=\langle\langle \psi_\alpha(x);\ \bar{\psi}_\beta(x')\rangle\rangle=-i\,\mathrm{Tr}\{\rho_G T[\psi_\alpha(x)\bar{\psi}_\beta(x')]\} =-i\,\mathrm{Tr}\{\rho_G[\psi_\alpha(x)\bar{\psi}_\beta(x')\theta(t-t') -\bar{\psi}_\beta(x')\psi_\alpha(x)\theta(t'-t)]\} , \quad (3)$$

where $\bar{\psi}=\psi^\dagger\gamma^0$, $\psi_\alpha(x)=\psi_\alpha(\mathbf{x},t)=e^{i\tilde{H}t}\psi_\alpha(\mathbf{x})e^{i\tilde{H}t}$ is the Heisenberg picture field operators; $\rho_G=\exp(\Omega-\beta\tilde{H})$ the grand canonical ensemble density matrix, and $\tilde{H}=\int d^3x\tilde{H}$ the Hamiltonian operator. The equation of motion of baryon Green's function is

$$i\frac{\partial}{\partial t}G_{\alpha\beta}(x-x')=\delta(t-t')\langle\{\psi_\alpha(x),\bar{\psi}_\beta(x')\}\rangle +\langle\langle[\psi_\alpha(x),\tilde{H}]_t;\ \bar{\psi}_\beta(x')\rangle\rangle . \quad (4)$$

Using Eq. (2), Eq. (4) becomes

$$(i\gamma_\mu\partial^\mu-M+\mu\gamma^0)G(x-x') =\delta(x-x')+g_v\gamma_\mu\langle\langle V^\mu(x)\psi(x);\ \bar{\psi}_\beta(x')\rangle\rangle -g_s\langle\langle\phi(x)\psi(x);\ \bar{\psi}(x')\rangle\rangle . \quad (5)$$

Obviously, if we introduce the first-order PC approximation as was done in a nonrelativistic case [9], replace the vector meson-baryon Green's function $\langle\langle V^\mu(x)\psi(x);\ \bar{\psi}(x')\rangle\rangle$ and the scalar meson-baryon Green's function $\langle\langle\phi(x)\psi(x);\bar{\psi}(x')\rangle\rangle$ in Eq. (5) as

$$\langle\langle V^\mu(x)\psi(x);\ \bar{\psi}(x')\rangle\rangle\approx V^0\delta_{\mu 0}\langle\langle\psi(x),\ \bar{\psi}(x')\rangle\rangle , \quad (6)$$

$$\langle\langle\phi(x)\psi(x);\ \bar{\psi}(x')\rangle\rangle\approx\phi_0\langle\langle\psi(x),\ \bar{\psi}(x')\rangle\rangle , \quad (7)$$

respectively, and solve the Green's function $G(x-x')$ by taking the Fourier transformation in Eq. (5), we will find the mean field results.

But if we want to discuss the fluctuation effects of scalar meson field, we cannot stay in the first-order step. We must consider the higher-order corrections. The equation of motion for scalar baryon Green's function $\langle\langle\phi(x)\psi(x);\ \bar{\psi}(x')\rangle\rangle$ is

$$(i\gamma_\mu\partial^\mu-M+\mu\gamma_0)\langle\langle\phi(x)\psi(x);\ \bar{\psi}(x')\rangle\rangle =\delta(x-x')\phi_0+g_v\gamma_\mu\langle\langle\phi(x)V^\mu(x)\psi(x);\ \bar{\psi}(x')\rangle\rangle -g_s\langle\langle\phi(x)\phi(x)\psi(x);\ \bar{\psi}(x')\rangle\rangle , \quad (8)$$

where $\phi_0=\langle\phi(x)\rangle$. A similar equation for vector meson-baryon Green's function is

$$(i\gamma_\mu\partial^\mu-M+\mu\gamma_0)\langle\langle V^\alpha(x)\psi(x);\ \bar{\psi}(x')\rangle\rangle =\delta(x-x')\delta^{\alpha 0}V^0+g_v\gamma_\mu\langle\langle V^\alpha(x)V^\mu(x)\psi(x);\ \bar{\psi}(x')\rangle\rangle -g_s\langle\langle V^\alpha(x)\phi(x)\psi(x);\ \bar{\psi}(x')\rangle\rangle , \quad (9)$$

where $V^0=\langle V^\mu(x)\rangle\delta^{\mu 0}$. In Eqs. (8) and (9) we have assumed that the meson fields $\phi(x)$, $V^\mu(x)$ change slowly with time and space and the terms including $\partial^\mu\phi,\partial^\mu V_\nu$ can be neglected.

Obviously, Eqs. (5), (8), and (9) do not form a closed set of equations for $\langle\langle\phi(x)\psi(x);\ \bar{\psi}(x')\rangle\rangle$, $\langle\langle V^\mu(x)\psi(x);\ \bar{\psi}(x')\rangle\rangle$, and $G(x-x')$. To make these equations closed, we introduce the second-order PC approximation and make replacements as follows:

$$\langle\langle\phi(x)\phi(x)\psi(x);\ \bar{\psi}(x')\rangle\rangle \approx\langle\phi(x)\phi(x)\rangle\langle\langle\psi(x);\ \bar{\psi}(x')\rangle\rangle , \quad (10)$$

$$\langle\langle V^\alpha(x)V^\mu(x)\psi(x);\ \bar{\psi}(x')\rangle\rangle \approx\langle V^\alpha(x)V^\mu(x)\rangle\langle\langle\psi(x);\ \bar{\psi}(x')\rangle\rangle\delta^{\alpha\mu} , \quad (11)$$

$$\langle\langle V^\alpha(x)\phi(x)\psi(x);\ \bar{\psi}(x')\rangle\rangle \approx\phi_0 V^0\delta^{\alpha 0}\langle\langle\psi(x);\ \bar{\psi}(x')\rangle\rangle . \quad (12)$$

Under this approximation, we get three self-consistent closed equations in energy momentum representation

$$(\gamma\cdot k+\gamma^0\mu-M)G(k)=1+g_v\gamma_\alpha D^\alpha(k)-g_s F(k) , \quad (13)$$

$$(\gamma\cdot k+\gamma^0\mu-M)F(k)=\phi_0+g_v\gamma_0\phi_0V_0F(k) -g_s\Phi^2G(k) , \quad (14)$$

$$(\gamma\cdot k+\gamma^0\mu-M)D^\alpha(k)=V_0\delta^{\alpha 0}+g_v\gamma_\lambda C^{\alpha\lambda}G(k) -g_s\phi_0V^0\delta^{\alpha 0}G(k) , \quad (15)$$

where $\Phi^2=\langle\phi(x)\phi(x')\rangle_{x'\to x}$; $C^{\alpha\lambda}=\langle V^\alpha(x)V^\lambda(x')\rangle_{x'\to x}$; $G(k)$, $F(k)$, and $D^\alpha(k)$ are the Fourier transforms of $G(x-x')$, $\langle\langle\phi(x)\psi(x);\ \bar{\psi}(x')\rangle\rangle$, and $\langle\langle V^\alpha(x)\phi(x)\psi(x);\ \bar{\psi}(x')\rangle\rangle$, respectively. After some calculations, we obtain the function $G(k)$, $F(k)$, and $D^\alpha(k)$ from Eqs. (13)–(15). The result for $G(k)$ is

$$G(k)=G_F(k)+G_D(k)\ , \tag{16}$$

$$G_F(k)=\frac{\gamma\cdot\tilde{k}+M-g_s\phi_0}{\tilde{k}_0^2-E^*(k)_1^2+i\epsilon}\ , \tag{17}$$

$$G_D(k)=\frac{i\pi}{2\Theta}\left[(\Theta+\phi_0)(\gamma\cdot\tilde{k}+M-g_s\Theta)\frac{1}{E^*(k)_1}\{\delta[\tilde{k}_0-E^*(k)_1]n_1+\delta[\tilde{k}_0+E^*(k)_1]\bar{n}_1\}\right.$$
$$\left.+(\Theta-\phi_0)(\gamma\cdot\tilde{k}+M+g_s\Theta)\frac{1}{E^*(k)_2}\{\delta[\tilde{k}_0-E^*(k)_2]n_2+\delta[\tilde{k}_0+E^*(k)_2]\bar{n}_2\}\right]\ , \tag{18}$$

where $\tilde{k}_0=k_0+\nu$, $\nu=\mu-g_v V_0$, $\tilde{\mathbf{k}}=\mathbf{k}$, and

$$\Theta=[\Phi^2-(g_v/g_s)^2(\langle V^\mu V_\mu\rangle-V_0^2)]^{1/2}\ , \tag{19}$$

$$n_1=\frac{1}{\exp(\beta[E^*(k)_1-\nu])+1},\quad \bar{n}_1=\frac{1}{\exp(\beta[E^*(k)_1+\nu])+1}\ , \tag{20}$$

$$n_2=\frac{1}{\exp(\beta[E^*(k)_2-\nu])+1},\quad \bar{n}_2=\frac{1}{\exp(\beta[E^*(k)_2+\nu])+1}\ , \tag{21}$$

$$E^*(k)_1=[\mathbf{k}^2+(M-g_s\Theta)^2]^{1/2},\quad E^*(k)_2=[\mathbf{k}^2+(M+g_s\Theta)^2]^{1/2}\ . \tag{22}$$

Furthermore, in order to find the scalar field correlation function Φ^2, we must consider the scalar meson Green's function. Define this Green's function as

$$\Delta(x-x')=\langle\langle\phi(x);\ \phi(x')\rangle\rangle=-i\,\mathrm{Tr}\{\rho_G[\theta(t-t')\phi(x)\phi(x')+\theta(t'-t)\phi(x')\phi(x)]\}\ . \tag{23}$$

On shifting the field

$$\phi=\phi_0+\phi'\ , \tag{24}$$

where $\phi_0=\langle\phi\rangle$ is the Gibbs ensemble average of scalar field

$$\phi_0=\frac{g_s}{m_s^2}\langle\bar{\psi}\psi\rangle \tag{25}$$

and ϕ' represents the thermal fluctuation effect of scalar meson field, we can calculate the fluctuation of scalar field:

$$\langle(\Delta\phi)^2\rangle=\langle\phi^2\rangle-\langle\phi\rangle^2=\Phi^2-\phi_0^2 \tag{26}$$

by $\Delta(x-x')$. Substituting Eq. (24) into the equation of motion of $\Delta(x-x')$ and using the same treatment as Ref. [9], we find the Green's function $\Delta(x-x')$ in energy-momentum representation as

$$\Delta(k)=\frac{1}{k^2-m_s^2+i\epsilon}-2\pi i n_s(k)\delta(k^2-m_s^2)+\frac{i m_s^2\phi_0^2(2\pi)^4\delta^4(k)}{k^2-m_s^2+i\epsilon}\ , \tag{27}$$

where

$$n_s(k)=\frac{1}{\exp[\beta(\mathbf{k}^2+m_s^2)^{1/2}]-1} \tag{28}$$

is the scalar meson distribution function. At zero temperature, $n_s(k)=0$, Eq. (27) reduces to that given by QHD with a "tadpole" diagram approximation [3]. The second term of the right-hand side of Eq. (27) comes from $\langle\phi'^2\rangle$ and represents the thermal fluctuation.

Similarly, the vector-meson Green's function can be found by the same procedure. The result is

$$D_{\mu\nu}(k)=\left[-g_{\mu\nu}+\frac{k_\mu k_\nu}{m_v^2}\right]\left[\frac{1}{k^2-m_v^2+i\epsilon}-2\pi i n_v(k)\delta(k^2-m_v^2)\right]+\frac{i m_v^2 V_0^2\delta_{\mu 0}\delta_{\nu 0}(2\pi)^4\delta^4(k)}{k^2-m_v^2+i\epsilon}\ , \tag{29}$$

where

$$n_v(k)=\frac{1}{\exp[\beta(\mathbf{k}^2+m_v^2)^{1/2}]-1} \tag{30}$$

and

$$V_0=\frac{g_v}{m_v^2}\langle\psi^\dagger\psi\rangle . \tag{31}$$

III. THERMODYNAMICAL QUANTITIES

Now we are in a position to calculate the thermodynamical quantities. It can easily be seen that the integrals of $G_F(k)$ are divergent and must be carried out by renormalization. This can be done by considering the vacuum fluctuations as in QHD [3]. An alternative treatment which had been taken in QHD is to drop all terms arising from integrals over $G_F(k)$ [3]. To leading order, the latter treatment, as was argued by one of the present authors [17], is inconsistent with large N_c QCD expansion. Hereafter we use the latter treatment and discuss the integrals that involved $G_D(k)$ only.

Using Green's functions given by Sec. II, and the correlation function formula [9]

$$\begin{aligned}F_{BA}(t-t')&=\langle B(t')A(t)\rangle\\&=i\int_{-\infty}^{\infty}\frac{G_{AB}(E+i0^+)-G_{AB}(E-i0^-)}{e^{\beta E}-\eta}\\&\quad\times e^{-iE(t-t')}dE ,\end{aligned} \tag{32}$$

where

$$G_{AB}(E)=\frac{1}{2\pi}\int_{-\infty}^{\infty}G_{AB}(t)e^{iEt}dt \tag{33}$$

is the Fourier transform of $G_{AB}(t)$, and $\eta=+1$ or $\eta=-1$ for boson or fermion, respectively. We find

$$\Phi^2=\langle\phi\phi\rangle=\phi_0^2+\frac{1}{(2\pi)^3}\int\frac{d^3\mathbf{k}}{(\mathbf{k}^2+m_s^2)^{1/2}}n_s(k) , \tag{34}$$

$$\langle V^\mu V_\mu\rangle=V_0^2-\frac{3}{(2\pi)^3}\int\frac{d^3\mathbf{k}}{(\mathbf{k}^2+m_v^2)^{1/2}}n_v(k) , \tag{35}$$

$$\rho=\rho_B=\langle\psi^\dagger\psi\rangle=\frac{\gamma}{2\Theta}\int\frac{d^3\mathbf{k}}{(2\pi)^3}[(\Theta+\phi_0)(n_1-\bar n)+(\Theta-\phi_0)(n_2-\bar n_2)] , \tag{36}$$

$$\rho_s=\langle\bar\psi\psi\rangle=\frac{\gamma}{2\Theta}\int\frac{d^3\mathbf{k}}{(2\pi)^3}\left[(\Theta+\phi_0)(M-g_s\Theta)\frac{1}{E^*(k)_1}(n_1+\bar n_1)+(\Theta-\phi_0)(M+g_s\Theta)\frac{1}{E^*(k)_2}(n_2+\bar n_2)\right] . \tag{37}$$

The energy density ϵ and the pressure p at a given temperature can be found by the ensemble average of energy-momentum tensor:

$$\begin{aligned}\epsilon&=\langle\hat T_v^{00}\rangle+\langle\hat T_s^{00}\rangle+\langle\hat T_B^{00}\rangle\\&=\tfrac12 m_v^2V_0^2+\tfrac12 m_s^2\phi_0^2+\int\frac{d^3\mathbf{k}}{(2\pi)^3}(\mathbf{k}^2+m_s^2)^{1/2}n_s(k)+\int\frac{d^3\mathbf{k}}{(2\pi)^3}(\mathbf{k}^2+m_v^2)^{1/2}n_v(k)\\&\quad+\frac{\gamma}{2\Theta}\int\frac{d^3\mathbf{k}}{(2\pi)^3}[(\Theta+\phi_0)E^*(k)_1(n_1+\bar n_1)+(\Theta-\phi_0)E^*(k)_2(n_2+\bar n_2)] ,\end{aligned} \tag{38}$$

$$\begin{aligned}p&=\tfrac13\langle\hat T_v^{ii}\rangle+\tfrac13\langle\hat T_s^{ii}\rangle+\tfrac13\langle\hat T_B^{ii}\rangle\\&=\tfrac12 m_v^2V_0^2-\tfrac12 m_s^2\phi_0^2+\tfrac13\int\frac{d^3\mathbf{k}}{(2\pi)^3}\frac{\mathbf{k}^2}{(\mathbf{k}^2+m_s^2)^{1/2}}n_s(k)+\int\frac{d^3\mathbf{k}}{(2\pi)^3}\frac{\mathbf{k}^2}{(\mathbf{k}^2+m_v^2)^{1/2}}n_v(k)\\&\quad+\frac{\gamma}{6\Theta}\int\frac{d^3\mathbf{k}}{(2\pi)^3}\left[(\Theta+\phi_0)\frac{\mathbf{k}^2}{E^*(k)_1}(n_1+\bar n_1)+(\Theta-\phi_0)\frac{\mathbf{k}^2}{E^*(k)_2}(n_2+\bar n_2)\right] .\end{aligned} \tag{39}$$

The effective mass of baryon is given by

$$M^*=M-g_s\Theta . \tag{40}$$

Equations (34)–(40) form a closed set of equations for calculating thermodynamical quantities self-consistently. The second term of the right-hand side of Eqs. (27) and (29) represents the fluctuation of meson fields $\langle\Delta\phi\rangle^2=\Phi^2-\phi_0^2$, $\langle(\Delta V_\mu)^2\rangle=\langle V_\mu^2\rangle-\langle V_\mu\rangle^2$. If we omit this term, our results will reduce to that given by the MFT. The equation of state for relativistic symmetric nuclear matter is given by Eq. (39). We can calculate the pressure-density isotherms from the above equations. The critical temperature KT_c and critical density ρ_c for a liquid-gas phase transition are determined by the condition

$$\left(\frac{\partial p}{\partial\rho}\right)_T=\left(\frac{\partial^2 p}{\partial\rho^2}\right)_T=0 . \tag{41}$$

Our results are summarized in Sec. IV.

IV. RESULTS AND DISCUSSIONS

Using the formulas given by Sec. III, we calculated the effective mass M^*, equation of state, and the saturation energy numerically. Our results are summarized in Figs. 1–7. The parameters in our calculations are chosen as $C_s^2=g_s^2(M^2/m_s^2)=267.1$, $C_v^2=g_v^2(M^2/m_v^2)=195.9$; $m_s=550.0$ MeV, $m_v=783.0$ MeV, which have been taken in QHD to reproduce the equilibrium properties of nuclear matter.

The M^*/M vs k_F^* curves for different temperatures [0 MeV (curve A), 100 MeV (curves B1 and B2), and 200 MeV (curves C1 and C2)] are shown in Fig. 1. Since $k_F^*=(6\pi^2\rho/\gamma)^{1/3}$, $\gamma=4$, the curve of M^*/M vs k_F^* describes the density dependences of effective mass of nucleon indeed. To illustrate the fluctuation effects of meson fields, we show the results calculated by our second-order PC theory (PCT) (solid curves) as well as by the MFT (dashed curves) simultaneously. We find that the fluctuation effects are considerable in low-density regions and small in high-density regions. As shown, the effective mass M^* given by the PCT is less than that given by the MFT for thermal excitations given by the second term of the right-hand sides of Eqs. (27) and (29). We also see from this figure that the discrepancy between the solid line and the dashed line for high temperatures is larger than that for low temperatures. It means that the fluctuation effects are important at high temperatures. To make our conclusion more transparent, we show the M^*/M vs kT curve for a fixed density ($\rho=0$) in Fig. 2. We find that the thermal fluctuation effects of the meson fields bring down the curve remarkably in high-temperature regions.

The saturation curves of relativistic nuclear matter for different temperatures are shown in Figs. 3–5. In low-temperature regions ($kT<20$ MeV), we show the results given by PCT in Fig. 3 only, because the differences between the correspondent results given by MFT and PCT are very small; the curves almost coincide since the parameters chosen in our calculation are just the parameters chosen by MFT and the saturation curve at zero temperature given by PCT is the same as that given by MFT. The experimental values of binding energy, equilibrium density, etc., can of course be explained by our theory. In Figs. 4 and 5 we see that the thermal fluctuation effects of meson fields on the saturation energy at high temperatures $KT=50$ MeV and 100 MeV are considerable, especially in the low-density regions. From these three figures we find that the saturation energy will

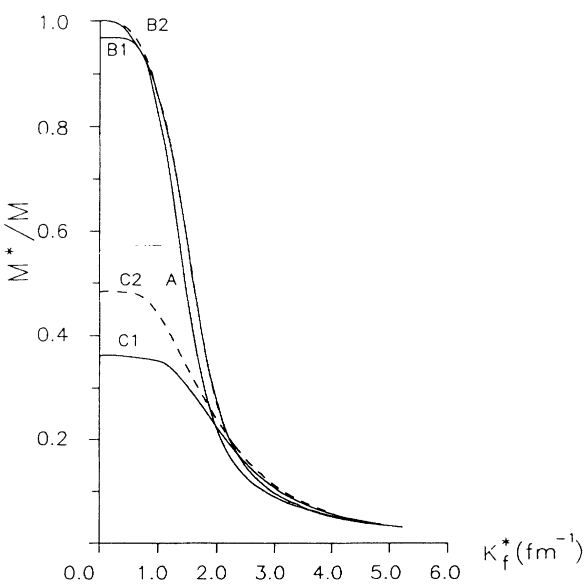

FIG. 1. Effective mass as a function of density. The dashed lines represent the results given by the mean field theory (MFT), and the solid lines for pair cutoff theory (PCT). Curves A, B, C correspond to $KT=0$ MeV, 100 MeV, 200 MeV, respectively.

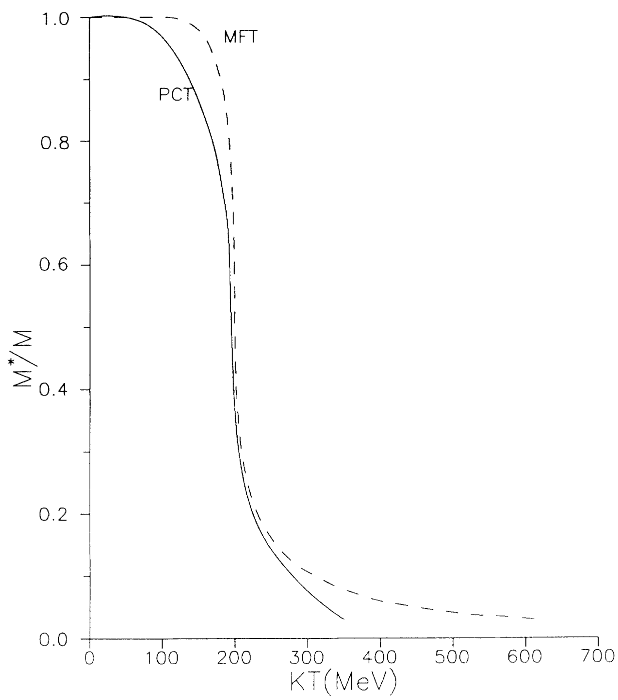

FIG. 2. Effective mass as a function of temperature for $\rho=0$.

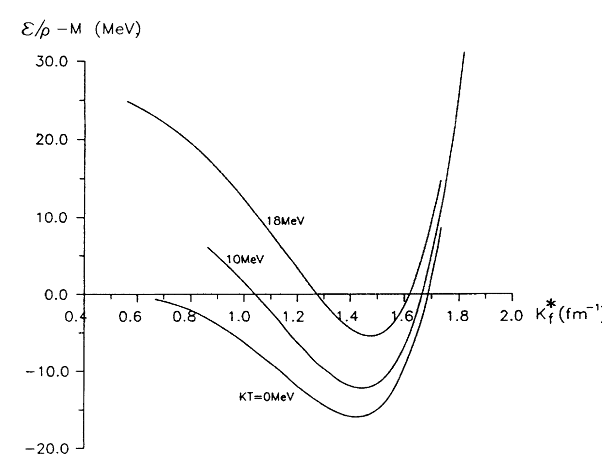

FIG. 3. Saturation curves of nuclear matter for various temperatures at $KT=0$, 10, and 18 MeV.

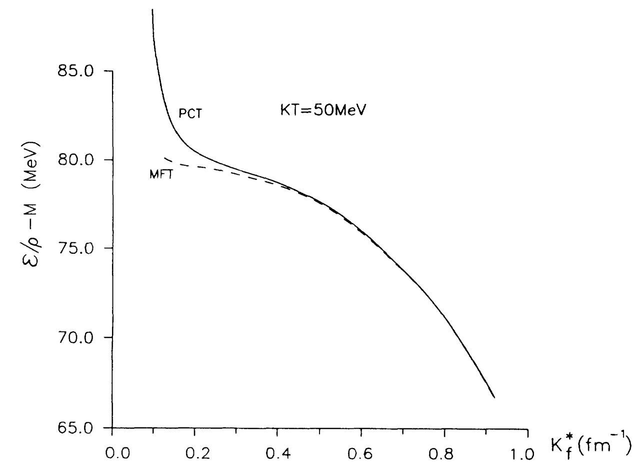

FIG. 4. Same as Fig. 3, except for $KT = 50$ MeV.

increase considerably as temperature increases, and the equilibrium density increases very slowly. This is of course very reasonable.

The pressure-density isotherms of relativistic nuclear matter are shown in Figs. 6 and 7. In Refs. [9,11,14], by employing the Skyrme interactions as well as Gogny interactions, we calculated the pressure-density isotherms for nonrelativistic nuclear matter. By using the same PC method given by the QHD-I model for relativistic nuclear matter and that given by Skyrme interactions as well as Gogny interactions for nonrelativistic nuclear matter, we see that the isotherms have generally the similar behavior. The shapes of isotherms look similar to each other, because all interactions (Skyrme interactions, Gogny interactions, or interactions of the QHD-I model) have the same typical forms as the Van der Waals interaction which determines the general behavior of liquid-gas isotherms.

Although the shapes of isotherms for relativistic nuclear matter and nonrelativistic nuclear matter look similar, the detail values of saturation density, saturation pressure, and the critical point are quite different. In fact, these values depend not only on the interactions of the nuclear matter, but also on the treatments whether the relativistic corrections, especially the fluctuation effects, are taken into account or not. To show the

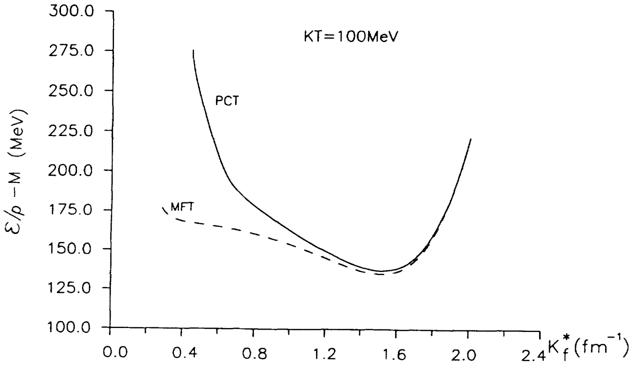

FIG. 5. Same as Fig. 3, except for $KT = 100$ MeV.

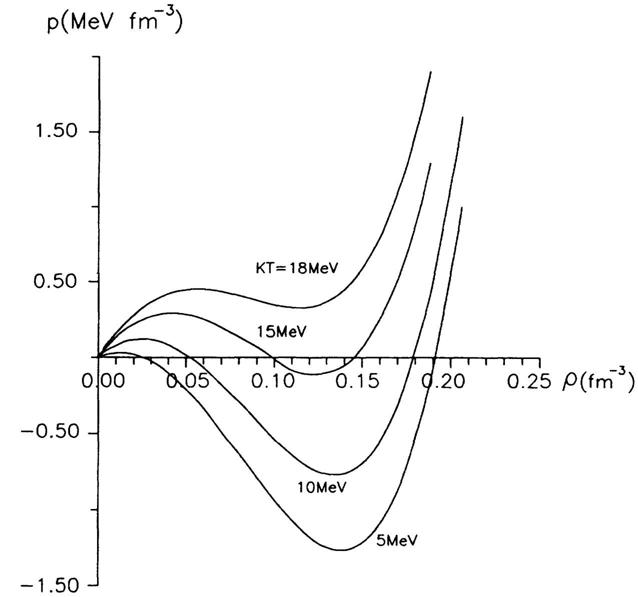

FIG. 6. Relativistic nuclear matter pressure-density isotherms.

thermal fluctuation effects of the meson fields transparently, we draw two isotherms, one corresponds to PCT and the other to MFT, in Fig. 7 for comparison. We find that the pressure given by PCT in low-density regions is larger than that given by MFT.

The critical point is determined by Eq. (32) and can be calculated numerically. The results are: critical temperature $KT_c = 20.56$ MeV, critical density $\rho_c = 0.087$ fm^{-3}, critical pressure $p_c = 0.643$ MeV fm^{-3}, and the effective mass at critical point $(M^*/M)_c = 0.781$.

In summary, we would like to point out that the fluctuation effects of meson fields are important in low-

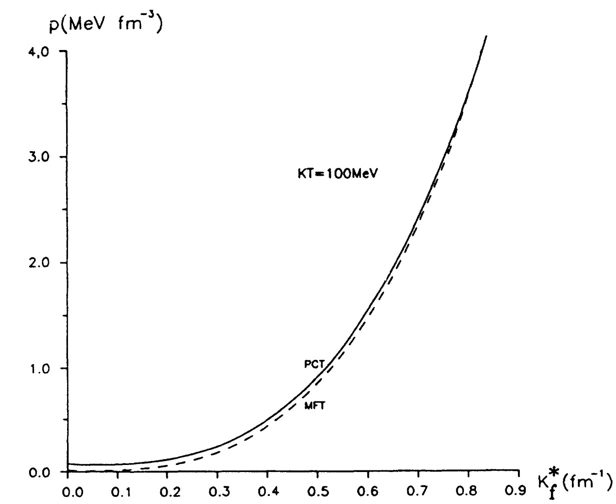

FIG. 7. Pressure-density isotherms at $KT = 100$ MeV for PCT and MFT.

density regions and/or high-temperature regions. The real-time finite-temperature Green's function method with pair cutoff approximation gives us a very useful tool to discuss the thermodynamical quantities as well as the fluctuation effects in both nonrelativistic and relativistic cases.

ACKNOWLEDGMENTS

This work was supported in part by the National Science Foundation of China under Grants No. 19175014 and by the Foundation of State Education Commission of China.

[1] L. S. Celenza and C. M. Shakin, *Relativistic Nuclear Physics: Theories of Structure and Scattering* (World Scientific, Singapore, 1988).

[2] S. A. Chin, Ann. Phys. (N.Y.) **108**, 301 (1977).

[3] B. D. Serot and J. D. Walecka, in *Advances in Nuclear Physics,* edited by J. W. Negele and E. Vogt (Plenum, New York, 1986), Vol. 16.

[4] J. W. Negele, Comments Nucl. Part. Phys. **14**, 303 (1985).

[5] G. E. Brown, Comments Nucl. Part. Phys. **17**, 39 (1987).

[6] R. J. Furnstahl and B. D. Serot, Phys. Rev. C **41**, 262 (1990); **43**, 105 (1991).

[7] J. A. McNeil, C. E. Price, and J. R. Shepard, Phys. Rev. C **42**, 2442 (1990).

[8] For example, L. E. Reichl, *A Modern Course in Statistical Physics* (University of Texas, Texas, 1980).

[9] R. K. Su, S. D. Yang, and T. T. S. Kuo, Phys. Rev. C **35**, 1539 (1987).

[10] R. K. Su, S. D. Yang, and T. T. S. Kuo, Phys. Rev. C **37**, 1770 (1988).

[11] R. K. Su and F. M. Lin, Phys. Rev. C **39**, 2438 (1989).

[12] R. K. Su and F. M. Lin, J. Phys. G **15**, 1591 (1989).

[13] R. K. Su, S. D. Yang, G. L. Li, and T. T. S. Kuo, Mod. Phys. Lett. A **1**, 71 (1986).

[14] H. Q. Song, G. T. Zheng, and R. K. Su, J. Phys. G **16**, 1861 (1990).

[15] H. Q. Song and R. K. Su, Phys. Rev. C **44**, 2505 (1991).

[16] For example, see R. K. Su and Z. Hu, Phys. Lett. A **141**, 420 (1989); **147**, 115 (1990); A. D. Linde, Rep. Prog. Phys. **42**, 390 (1979).

[17] R. K. Su, in *Quark-Gluon Structure of Hadrons and Nuclei, Proceedings of the International Workshop,* edited by L. S. Kisslinger and X. Qiu (International Academy, Beijing Pub., 1991), p. 258.